The force awakens — the 750 GeV diphoton excess at the LHC from a varying electromagnetic coupling

Ulf Danielsson,[*] Rikard Enberg,[†] Gunnar Ingelman,[‡] and Tanumoy Mandal[§]

Department of Physics and Astronomy,

Uppsala University, Box 516, SE-751 20 Uppsala, Sweden

(Dated: January 5, 2016)

Abstract

We show that the recent 750 GeV diphoton excess observed at the LHC may be explained by the production of a scalar of the type involved in Bekenstein's framework for varying-α theories, with the difference that the scalar in our model has a large mass. The model has only two free parameters, the mass of the scalar and the scale of this new physics, which are fixed by the LHC excess to 750 GeV and $3 - 4$ TeV, respectively. We discuss collider and cosmology aspects of the model, and give predictions for future LHC searches. In particular, the scalar is dominantly produced by quark-antiquark fusion in association with a photon or a fermion pair. In addition, it can be produced in the s-channel in photon-photon fusion. Its dominating decay is to diphotons, but it also has a large three-body decay to a fermion pair and a photon, which provides an interesting search channel with a dilepton-photon resonance at 750 GeV. We also comment on the possibility that the new physics is related to extra dimensions or string theory.

[*]Electronic address: ulf.danielsson@physics.uu.se

[†]Electronic address: rikard.enberg@physics.uu.se

[‡]Electronic address: gunnar.ingelman@physics.uu.se

[§]Electronic address: tanumoy.mandal@physics.uu.se

arXiv:1601.00624v1 [hep-ph] 4 Jan 2016

I.   INTRODUCTION

Recently both the ATLAS and the CMS collaborations reported excesses in the dipho-
ton invariant mass distribution around 750 GeV [1, 2] based on the 13 TeV data from
Run 2. The excesses have local significances of 3.9σ for ATLAS and 2.0σ for CMS for a
relatively large width of the resonance (up to 45 GeV for ATLAS) or 3.6σ for ATLAS and
2.6σ for CMS for a narrow width resonance. Thus ATLAS has a slightly larger signifi-
cance for a large width while CMS has a slightly larger significance for a narrow width.
Including the look-elsewhere effect, the global significances are further reduced. The mass
of the resonance is near 750 GeV, which is the value we will assume in this paper. The
results are thus not statistically significant enough to draw definite conclusions, but are
nevertheless very interesting to try to understand from a theoretical perspective.

In this paper we propose to explain the observed excess by a massive scalar that
decays into a pair of photons. This scalar is associated with a model for a space-time
varying electromagnetic coupling constant, constructed more than thirty years ago by
Jacob Bekenstein [3, 4]. Bekenstein's model is the first consistent such model—it is
Lorentz, gauge and time-reversal invariant and respects causality. The original motivation
was to accommodate possible variations of the fine-structure constant over cosmological
scales, but despite careful searches such variations have not been detected, see e.g. [5].

In string theory all couplings are associated with scalar fields, called moduli, and are
thus subject to variations. The excitations of these fields are typically very heavy and
as a consequence the couplings will be locked to essentially constant values, given by the
specific compactification scenario, see e.g. [6] for a discussion. The Bekenstein model is
not derived from string theory, but we consider it the simplest consistent scenario for
associating couplings with scalar fields.

In this paper we assume that the diphoton excess can be explained by a massive scalar
of the type appearing in the Bekenstein model. However, with such a high mass the fine-
structure constant will remain constant throughout most of the history of the universe
and no deviations would have been detectable so far.[1] The diphoton excess would then

---

[1] The new scalar should also be investigated as a candidate for the inflaton. The quadratic contribution
to the potential, with the 750 GeV mass, cannot be used for inflation, but one might consider higher
order terms providing a useful shape.

be the first hint that the fine-structure constant can vary if the energy is high enough.

As we will see, our model is qualitatively different from many proposed explanations of the LHC diphoton excess (see e.g. [7–13]) in that the resonance is not produced in the s-channel, but always together with either a photon, or with a dijet or dilepton pair (some recent papers discuss similar not pure s-channel processes, see e.g. [7, 14–16]). It may be, however, that the extra particles escape detection so that the production looks like an s-channel process in the detector. Moreover, the production is dominantly due to quark-antiquark fusion, with the gluon-gluon fusion production mode loop-suppressed in comparison to the quark-antiquark mode. Finally, no additional particles apart from the scalar are introduced.

This paper is organized as follows. In Section II we introduce the model and derive the interactions of the new scalar. In Section III and Section IV we discuss the phenomenology of the model, and through detailed numerical comparison with LHC data we extract the values of the two parameters in the model, resulting in a possible interpretation of the LHC diphoton excess as resulting from a scalar of the Bekenstein type. In Section V we conclude by considering the results in a larger context.

II.   THE MODEL

In the Bekenstein model [3, 4] the variation of the coupling constant e is derived from an action that reduces to electromagnetism for constant coupling. It is assumed that the space-time variation of the electromagnetic coupling is given by $e = e_0 \epsilon(x)$, where $\epsilon(x)$ is a scalar field with dynamics given by the kinetic term

$$\frac{1}{2} \frac{\Lambda^2}{\epsilon^2} (\partial_\mu \epsilon)^2, \tag{1}$$

where Λ is an energy scale. It is assumed that the field ϵ multiplies the electric charge e everywhere in the Lagrangian of the model. Specifically, this means that eA_μ is everywhere replaced by $e_0 \epsilon A_\mu$. Gauge invariance, and invariance with respect to a rescaling of ϵ, then requires that the field strength tensor be given by

$$F_{\mu\nu} = \frac{1}{\epsilon} \left[\partial_\mu (\epsilon A_\nu) - \partial_\nu (\epsilon A_\mu) \right]. \tag{2}$$

To keep our notation as explicit as possible we define $\widehat{F}_{\mu\nu} = \partial_\mu A_\nu - \partial_\nu A_\mu$, and introduce a scalar field φ such that $\epsilon = e^\varphi$. We will be assuming small fields, working at lowest

order, and therefore write $\epsilon \simeq 1 + \varphi$, and keep only terms linear in φ. We then find, for the kinetic term of the electromagnetic field, that $F_{\mu\nu}F^{\mu\nu} = \widehat{F}_{\mu\nu}\widehat{F}^{\mu\nu} - 2\varphi\widehat{F}_{\mu\nu}\widehat{F}^{\mu\nu}$. Finally, we define a new field $\phi = \varphi\Lambda$ so that all fields have their usual mass dimensions. In this way we find a Lagrangian for electromagnetism plus the scalar field given by

$$\mathcal{L} \supset \frac{1}{2}(\partial_\mu \phi)^2 - \frac{1}{4}\widehat{F}_{\mu\nu}\widehat{F}^{\mu\nu} + \frac{1}{2\Lambda}\phi\widehat{F}_{\mu\nu}\widehat{F}^{\mu\nu}. \tag{3}$$

Note that we have made a partial integration in the last term, and made use of the equation of motion for the electromagnetic field to lowest order in ϕ. This is the standard effective Lagrangian for a massless scalar field coupled to electromagnetism, with the scale of new physics given by Λ.

Because of the definition of e, the new scalar field ϕ will in addition to the interaction in Eq. (3) couple to all electrically charged fields. The coupling of the electromagnetic field to charged fermions is obtained from the covariant derivative, which is given by $D_\mu = \partial_\mu - ieQA_\mu$, where Q is the charge of the coupled field, and $e = e_0\epsilon$ so that $D_\mu = \partial_\mu - ie_0QA_\mu - ie_0Q(\phi/\Lambda)A_\mu$. If we now define $\widehat{D}_\mu = \partial_\mu - ie_0QA_\mu$ as the more familiar covariant derivative of electromagnetism, the gauge invariant kinetic term for fermions is given by

$$\mathcal{L} \supset i\overline{\psi}\slashed{D}\psi = i\overline{\psi}\widehat{\slashed{D}}\psi + \frac{e_0Q}{\Lambda}\phi\,\overline{\psi}\gamma^\mu\psi\,A_\mu. \tag{4}$$

The final interaction of ϕ to consider is the coupling to $W^\pm$ bosons, which is obtained by inserting $eA_\mu = e_0\epsilon A_\mu$ in the electroweak gauge kinetic term written in terms of the mass eigenstates. The resulting terms to lowest order in the electric coupling are shown below in Eq. (5).

As we have described above, this model has been used as a framework for a space-time varying fine-structure constant with a massless or very light scalar field ϕ. We will now add one new ingredient: a mass term for the scalar field with $m \sim 750$ GeV. The energy cost of moving ϕ away from its minimum will then be very large for energies $\lesssim m$, so that α_{EM} will have negligible variation.

To get the Lagrangian in its final form, let us now drop the hats on the above expressions, so that from now on, $F_{\mu\nu}$ is the standard field strength tensor. Collecting all terms,
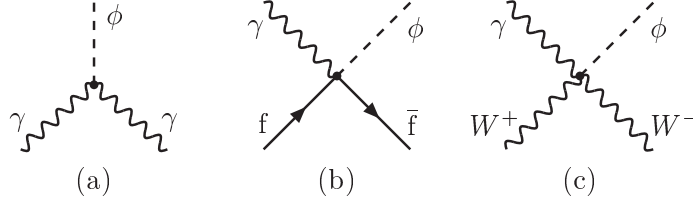
FIG. 1: Basic interaction vertices of the scalar field ϕ as given by the Lagrangian in Eq. (5).

we then have the Lagrangian of our model

$$\mathcal{L} = \mathcal{L}_{\text{SM}} + \frac{1}{2}(\partial_\mu \phi)^2 - \frac{1}{2}m^2\phi^2 + \frac{1}{2\Lambda}\phi F_{\mu\nu}F^{\mu\nu} + \frac{e_0 Q}{\Lambda}\phi \overline{\psi}\gamma^\mu\psi A_\mu$$
$$+ \frac{ie_0}{\Lambda}\phi\left[(\partial_\mu W_\nu^+ - \partial_\nu W_\mu^+)W^{-\mu}A^\nu - (\partial_\mu W_\nu^- - \partial_\nu W_\mu^-)W^{+\mu}A^\nu + F^{\mu\nu}W_\mu^+ W_\nu^-\right]$$
$$+ \frac{ie_0}{\Lambda}\left[(A_\nu\partial_\mu\phi - A_\mu\partial_\nu\phi)W_\mu^+ W_\nu^-\right], \tag{5}$$

where $\mathcal{L}_{\text{SM}}$ represents the ordinary Standard Model Lagrangian, and ψ is a generic field with charge Q denoting all electrically charged fermions of the Standard Model, written as Dirac spinors for both left- and right-handed components. Thus our model has only two new parameters, the mass m and the scale Λ. Note that the electromagnetic coupling e_0 in Eq. (5) is the usual not varying coupling, and the dynamics of the varying constant now sit instead in the scalar field ϕ.[2]

The last three terms in Eq. (5) are interaction terms. The vertices are shown in Fig. 1 and the corresponding Feynman rules are

$$\text{Fig. 1a} \quad : \quad \gamma\gamma\phi \quad \rightarrow \quad \frac{2i}{\Lambda}\left(p_{1\mu}p_{2\nu} - g_{\mu\nu}\,p_1 \cdot p_2\right) \tag{6}$$

$$\text{Fig. 1b} \quad : \quad \text{f}\bar{\text{f}}\gamma\phi \quad \rightarrow \quad \frac{ie_0 Q}{\Lambda}\gamma^\mu \tag{7}$$

$$\text{Fig. 1c} \quad : \quad \gamma\phi W^+ W^- \rightarrow \frac{ie_0}{\Lambda}\left(p_1^{\mu_3}g_{\mu_1,\mu_4} - p_1^{\mu_4}g_{\mu_1,\mu_3} + p_2^{\mu_3}g_{\mu_1,\mu_4} - p_2^{\mu_4}g_{\mu_1,\mu_3}\right.$$
$$\left. + p_3^{\mu_4}g_{\mu_1,\mu_3} - p_3^{\mu_1}g_{\mu_3,\mu_4} + p_4^{\mu_1}g_{\mu_3,\mu_4} - p_4^{\mu_3}g_{\mu_1,\mu_4}\right), \tag{8}$$

where in (6) and (8) the numbered indices refer to the particles in the order listed.

For simplicity, we have only let the electromagnetic coupling e vary. This has the consequence that only the photon and the fields carrying electric charge couple to ϕ. If

---

[2] For example, at very high energies above the mass of ϕ, small variations of the coupling constant e could become visible in e^+e^- collisions at a future linear collider. In the formulation here, where we have the fixed constant e_0, such variations would be associated with loops or real or virtual emission diagrams involving ϕ.

we instead let the $U(1)_Y$ hypercharge coupling vary, there will be additional couplings between the Z^0 boson and ϕ. It is also possible to let the other gauge couplings vary, but this adds even more structure, and since we are interested in the simplest possible model that can explain the diphoton excess, we leave the generalization for future work [17]. We note, however, that the Bekenstein model has been generalized [18] to vary the $SU(2)_L$ and $U(1)_Y$ couplings of the electroweak theory, either with both couplings varying in the same way, or independent of each other. In the latter case, there will be two scalar fields instead of one. In both cases the masses of the electroweak gauge bosons $W^\pm$ and Z^0 will also vary.

We are now ready to go on and investigate the phenomenology of the model with respect to the diphoton excess. We leave the study of further phenomenological aspects of the model for future work [17].

III.   PRODUCTION AND DECAYS AT THE LHC

In this section we study the LHC phenomenology of our model and derive limits on the scale Λ from the relevant LHC 8 TeV and 13 TeV diphoton resonance search results. We implement the Lagrangian shown in Eq. 5 in FEYNRULES2.0 [19] to generate the model files for the MADGRAPH5 [20] event generator. We use CTEQ6L1 [21] parton distribution functions (PDF) to compute cross sections. Detector simulation is performed for ATLAS and CMS using DELPHES 3.3.1 [22] which uses the FASTJET [23] package for jet clustering using the anti-k_T algorithm [24] with $R = 0.4$. We fix the mass of ϕ at 750 GeV for all our numerical computations.
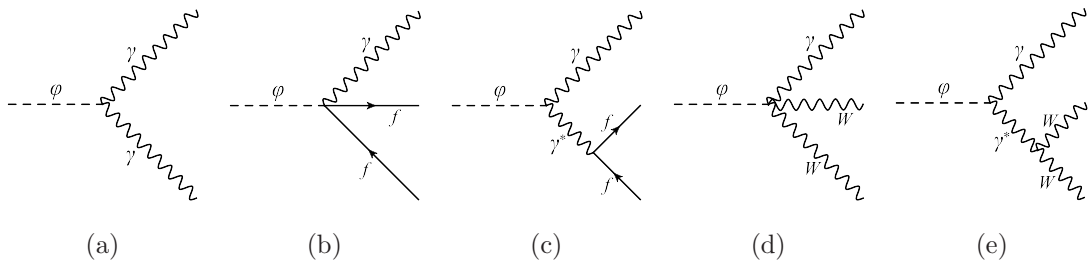

FIG. 2: The Feynman diagrams of the two and three body decay modes of ϕ.

Since ϕ originates from the variation of the fine-structure constant, it either directly couples to two photons or to the $\gamma\psi^+\psi^-$ type vertex (where ψ is any charged particle).

This leads to some new unconventional decay modes of ϕ unlike the SM-like Higgs boson. The only possible two-body decay of ϕ is the diphoton mode, which is a tree level decay— not a loop-induced decay through any charged particle. In Fig. 2, we show the Feynman diagrams of all possible two and three body decay modes of ϕ. Apart from these modes, there are other subdominant four-body decay modes (*e.g.* $\phi \to \gamma\psi^+\psi^{-*} \to \gamma\gamma\psi^+\psi^-$) possible for ϕ. In Table I, we show the partial widths and branching ratios (BR) of ϕ into its two, three and four body decay modes for $\Lambda = 1$ TeV. It is important to note that the branching ratios of ϕ are independent of Λ. From Table I, we can see that $\phi \to \gamma\gamma$ is the dominant decay mode and this mode has a branching ratio of about 70%. Due to the large width in the diphoton mode, ϕ might be a good candidate to explain the recent 750 GeV diphoton excess at the LHC. Moreover, the nonobservation of any excess expected in other channels from a SM-like scalar can also be explained as other decays of ϕ are not SM-like. To confirm the presence of ϕ or to set limit on Λ, we need dedicated analyses for other important channels that are not yet searched for at colliders.

Decay Mode	$\phi \to \gamma\gamma$	$\phi \to \gamma f f(jj)$	$\phi \to \gamma\gamma f f$	$\phi \to \gamma WW$	$\phi \to \gamma\gamma WW$	Total
Width (GeV)	8.393	2.666 (1.554)	0.554	0.280	0.019	11.91
BR (%)	70.46	22.38 (13.05)	4.65	2.35	0.16	-

TABLE I: The partial widths and branching ratios of ϕ for $m = 750$ GeV. The widths are proportional to Λ^{-2} and are here given for $\Lambda = 1$ TeV, whereas the BRs are independent of Λ. Here f includes all SM charged fermions and j denotes jets of "light" quarks, including b. The four-body final states are non-negligible corrections to the three-body modes.
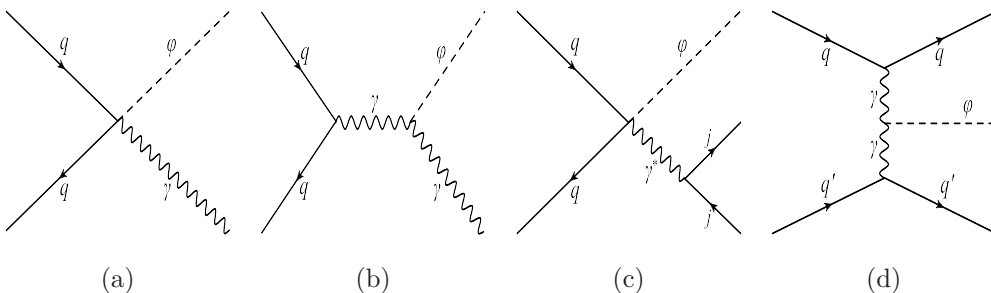

FIG. 3: Sample Feynman diagrams of the production of ϕ at the LHC.

In Fig. 3, we show a few sample Feynman diagrams of the two main production channels of ϕ at the LHC. Unlike the gg initiated SM-like Higgs boson production, these

7

Production mode	$\phi\gamma$	$\phi\gamma j$	$\phi\gamma jj$	ϕjj	$\gamma\gamma \to \phi$	$\phi\ell\ell$	$\phi\gamma W$	$\phi\gamma WW$	$\phi\gamma\gamma$	$\phi\gamma\ell\ell$
CS@8TeV (fb)	16.53	8.041	3.353	17.69	30.84	0.339	0.410	0.835	0.181	0.008
CS@13TeV (fb)	66.27	39.08	20.08	69.87	77.59	1.407	3.140	21.43	0.848	0.042

TABLE II: Partonic cross sections of various production channels of ϕ for $\Lambda = 1$ TeV computed at renormalization (μ_R) and factorization (μ_F) scales $\mu_R = \mu_F = m = 750$ GeV for LHC at 8 and 13 TeV. These cross sections are computed using CTEQ6L1 PDFs by applying some basic generation level cuts as defined in Eq. (9). Here, j denotes light jets including b-jet and ℓ includes $e^{\pm}$ and $\mu^{\pm}$. In the $\gamma\gamma \to \phi$ mode, the two initial γs come from photon pdf's. Note that all signal cross sections scale as Λ^{-2}.

channels are induced by a qq initial state. Therefore, to produce a TeV-scale ϕ one would get comparatively bigger contributions due to quark-PDFs at high-x than gluon-PDF. In Table II, we present the partonic cross sections of various production modes of ϕ for the 8 and 13 TeV LHC.

IV. COMPARISON TO THE LHC DATA

To compute these cross sections we apply the following basic kinematical cuts at the generation level wherever they are applicable.

$$p_T(x) > 25 \text{ GeV}; \quad |\eta(x)| < 2.5; \quad \Delta R(x,y) > 0.4 \quad \text{where} \quad x, y \equiv \{\gamma, \ell, j\} \tag{9}$$

The inclusive $pp \to \phi\gamma + $ jets, $pp \to \phi jj$ and $pp \to \phi pp$ are the three main production modes of ϕ. The exclusive production of ϕ i.e. $pp \to \phi pp$, where two forward protons are tagged, is an interesting process to search for, but this is beyond the scope of this paper (this production mode has been considered in [25–27], for models very different from ours). To estimate the inclusive $pp \to \phi\gamma$ signal without double counting, we use the MLM matching prescription used in MADGRAPH5 to match matrix element partons with the parton shower. Our inclusive signal includes up to two jets and we generate it by combining the following processes,

$$\left.\begin{aligned} pp &\to (\phi\,\gamma) &&\to \widehat{\gamma\gamma}\,\gamma\,, \\ pp &\to (\phi\,\gamma j) &&\to \widehat{\gamma\gamma}\,\gamma j\,, \\ pp &\to (\phi\,\gamma jj) &&\to \widehat{\gamma\gamma}\,\gamma jj\,. \end{aligned}\right\} \tag{10}$$

where we set the matching scale $Q_{cut} = 30$ GeV. Here, the curved connection above two photons signify that they come from the decay of ϕ. The matched cross section of the inclusive (up to 2-jets) $pp \to \phi\gamma + $ jets process is roughly 61 (12) fb for 13 (8) TeV LHC and it includes $\phi \to \gamma\gamma$ branching ratio. The two photons coming from ϕ-decay are relatively hard compared to the third photon. In Figs. 4a and 4b, we show the transverse momentum (p_T) distributions of the first and second hardest photons respectively. Since they come from the decay of a particle with mass 750 GeV, the p_T distributions of them roughly peak around 375 GeV. We show the p_T distribution of the third hardest photon in Fig. 4c. As expected, the invariant mass (M) distribution of the first and second hardest photons peaks at 750 GeV. This has been demonstrated in Fig. 4d.
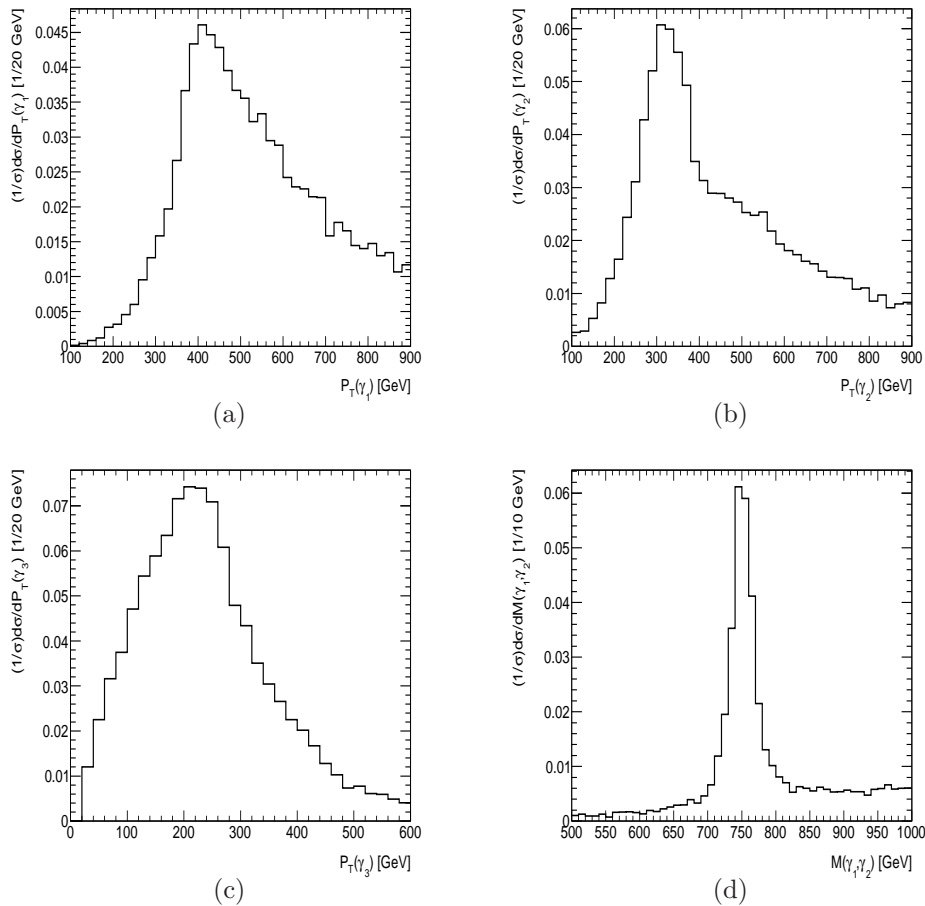

FIG. 4: Transverse momentum (p_T) and invariant mass (M) distributions of the selected photons by applying selection cuts used by 13 TeV CMS [2] analysis for the inclusive $\phi\gamma + $ jets channel. The p_T distributions of the three p_T-ordered photons shown in (a), (b) and (c) respectively. In (d) we show the invariant mass distribution of the two hardest photons.

9

The experimental searches for a high mass diphoton resonance, where the signal is an s-channel spin-0 or spin-2 resonance decaying to diphoton generally demand exactly two selected photons with no selected jet, whereas for inclusive diphoton resonance searches, one keeps events with at least two selected photons and any number of selected jets. All these searches are optimized for s-channel resonances decaying to two photons. Although there is no s-channel resonance production of ϕ present in our case, the two channels of inclusive $pp \to \phi\gamma \to 3\gamma$ and $pp \to \phi jj \to \gamma\gamma jj$ contribute most to the ATLAS [1] and CMS [2] analyses.

Now we want to investigate how selection cut efficiencies depend on the selection criteria imposed. In Table III, we show cut efficiencies for different selection criteria on the number of photons and jets for the inclusive $pp \to \phi\gamma \to 3\gamma$ and $pp \to \phi jj \to \gamma\gamma jj$ channels at the 13 TeV LHC.

We roughly employ the selection cuts used by ATLAS [1] and CMS [2] for their 13 TeV analysis as listed below. Although they have not mentioned any jet selection, we include basic jet selection cuts in the following list to demonstrate how our signal cut efficiencies change with different number of selected photons and jets. In Table III we show cut efficiencies for various selection categories for the two major contributing ϕ production channels, *viz.* inclusive (up to 2-jets) $pp \to \phi\gamma \to 3\gamma$ and $pp \to \phi jj \to \gamma\gamma jj$.

- Selection cuts for CMS 13 TeV analysis:

    1. Transverse momentum of selected photons or jets satisfy $p_T(\gamma), p_T(j) > 25$ GeV with two hardest photons satisfying $p_T(\gamma_1), p_T(\gamma_2) > 75$ GeV.

    2. Pseudorapidity of selected photons or jets satisfy $|\eta(\gamma)|, |\eta(j)| < 2.5$. For photons we exclude the barrel-endcap region by $1.44 < |\eta(\gamma)| < 1.57$.

    3. Separation in η-ϕ plane between any two photons or photon-jet pair satisfy $\Delta R(\gamma, \gamma), \Delta R(\gamma, j) > 0.4$.

    4. Invariant mass of the two hardest photons satisfy $M(\gamma_1, \gamma_2) > 230$ GeV.

- Selection cuts for ATLAS 13 TeV analysis:

    1. Transverse momentum of selected photons or jets satisfy $p_T(\gamma), p_T(j) > 25$ GeV

2. Pseudorapidity of selected photons or jets satisfy $|\eta(\gamma)| < 2.37$ and $|\eta(j)| < 2.5$.

3. Separation in η-ϕ plane between any two photons or photon-jet pair satisfy $\Delta R(\gamma, \gamma), \Delta R(\gamma, j) > 0.4$.

4. Invariant mass of the two hardest photons and their transverse momenta satisfy the relations $p_T(\gamma_1)/M(\gamma_1, \gamma_2) > 0.4$ and $p_T(\gamma_2)/M(\gamma_1, \gamma_2) > 0.3$.

Category	$2\gamma + 0j$	$\geq 2\gamma + 0j$	$2\gamma + \geq 0j$	$2\gamma + 1j$	$2\gamma + 2j$	$3\gamma + \geq 0j$	$\geq 2\gamma + \geq 0j$
ATLAS ($\phi\gamma$)	0.008	0.281	0.149	0.058	0.043	0.625	0.780
ATLAS (ϕjj)	0.0006	0.0007	0.543	0.041	0.214	0.009	0.553
CMS ($\phi\gamma$)	0.038	0.320	0.259	0.096	0.066	0.682	0.948
CMS (ϕjj)	0.0007	0.0008	0.749	0.051	0.293	0.012	0.762

TABLE III: Cut efficiencies for different selection criteria on the number of selected photons and jets for ATLAS [1] and CMS [2] diphoton resonance searches. Here, "$\phi\gamma$" and "ϕjj" mean inclusive (up to 2-jets) $pp \to \phi\gamma \to 3\gamma$ and $pp \to \phi jj \to \gamma\gamma jj$ processes respectively.

In Table III, it is evident that the cut efficiencies are highly dependent on the selection criteria. For example, if we demand exactly two selected photons and no selected jet (*i.e.* $2\gamma + 0j$), the cut efficiency is 0.038 for CMS($\phi\gamma$). On the other hand, this becomes 0.259 when we select two photons and any number of jets (*i.e.* $2\gamma + \geq 0j$). This is in contrast to the case of an *s*-channel production of SM-like scalar decays to two photons, where we should not expect drastically different cut efficiencies for $2\gamma + 0j$ and $2\gamma + \geq 0j$ selection categories. In order to derive a limit on Λ by recasting the $\sigma \times$ BR upper limit from an experiment, we need to properly take care of the cut efficiencies. This can be done by using the following relation:

$$\mathcal{N}_s = \sigma_s \times \epsilon_s \times \mathcal{L} = \left(\sum_i \sigma_i \times \epsilon_i \right) \times \mathcal{L} \, , \tag{11}$$

where $\mathcal{N}_s$ is the number of events for the signal considered and σ_s is the corresponding signal cross section for luminosity $\mathcal{L}$. The corresponding signal cut efficiency is denoted by ϵ_s. When different types of signal topology and/or final state contribute to any experimental observable, $\mathcal{N}_s$ can be expressed by the sum $\left(\sum_i \sigma_i \times \epsilon_i \right) \times \mathcal{L}$. Here, i runs

over all contributing signal processes to any observable. In our case, the following two processes contribute most to the s-channel diphoton resonance searches at the LHC:

$$\text{Process I } (p_1): \ pp \to \phi\gamma \to 3\gamma + \text{jets}; \quad \text{Process II } (p_2): \ pp \to \phi jj \to \gamma\gamma jj. \quad (12)$$

Therefore, in our case $\mathcal{N}_s = \Lambda^{-2} \times (\sigma_{p_1} \times \epsilon_{p_1} + \sigma_{p_2} \times \epsilon_{p_2})_{\Lambda=1 \text{ TeV}} \times \mathcal{L}$. Here, σ_{p_i} is the signal cross section for the i-th process and the corresponding signal efficiency is ϵ_{p_i}. We briefly mention about the relevant diphoton resonance searches at the LHC. For those experiments, we also estimate the lower limit on Λ by recasting the observed upper limit (UL) on $\sigma \times$ BR with the help of the relation given in Eq. 11.

Now we turn to the LHC run-I data related to the diphoton resonance searches [28–30]. All these experiments search for either a spin-0 or spin-2 object produced as an s-channel resonance and decays to two photons. We collect the observed UL on the cross sections and the corresponding efficiencies for resonance mass around 750 GeV for each experiment. We estimate the cut efficiencies for processes p_1 and p_2 for these experiments by employing selection cuts in the detector simulator DELPHES3.3.1. From all these information, one can estimate the lower limit (LL) on Λ from the formula given in Eq. 11. The overall result of the 8 TeV data of ATLAS and CMS set an upper limit of the cross section in the range 1-2 fb. Using this we can extract a lower limit of Λ for our model. This depends, however, on how the data is characterized in terms of number of photons and jets, since that affects the relevant efficiencies ϵ. Without reporting all numerical details here, we conclude that for the interpretation of the data as $2\gamma + 0j$, we obtain a lower limit of Λ in the range 0.5-1.5 TeV. Choosing instead $2\gamma+ \geq 0j$ would, however, give a lower limit Λ in the range 2.5-4 TeV.

There are two other relevant experiments at the 8 TeV LHC by ATLAS with $\mathcal{L} = 20.3$ fb^{-1} which are important to mention in this context. In [31], the diphoton resonance is searched for mass up to 600 GeV for the $2\gamma + 0j$ category. The UL on the cross section is set at roughly 1 fb around a mass of 600 GeV with cut efficiency roughly 70%. If we assume that we get a similar cross section UL for 750 GeV too, and the cut efficiency would remain similar, we get the LL, $\Lambda \gtrsim 0.43$ TeV. In [32], a triphoton resonance is searched for by ATLAS. This analysis is limited up to a resonance mass of 500 GeV. In our model, there is a possibility of a three photon final state originating from $pp \to \phi\gamma \to 3\gamma$ (although not a triphoton resonance), and therefore, triphoton resonance searches can

Experiment	σ_s (fb)	ϵ_s	σ_{p_1} (fb)	ϵ_{p_1}	σ_{p_2} (fb)	ϵ_{p_2}	Λ (C1)	Λ (C2)
ATLAS@13TeV, 3.2 fb^{-1} [1]	10.5	0.4	61.2	0.15	47.1	0.54	2.9	4.2
CMS@13TeV, 2.6 fb^{-1} [2]	17.0	0.3	61.2	0.26	47.1	0.75	3.2	4.3

TABLE IV: The observed UL on cross sections, σ_s and corresponding efficiencies, ϵ_s for mass around 750 GeV. In the last two columns we show the derived value of Λ for $m = 750$ GeV for the selection categories C1: $2\gamma+ \geq 0j$ and C2: $\geq 2\gamma+ \geq 0j$.

also be used to set limits on our model parameters in the future, if the analysis extends the resonance mass range beyond 750 GeV.

Let us now turn to the 13 TeV data, where a more pronounced hint for an excess can give more precise information regarding our model. Following the same method as used to derive limits on Λ from the 8 TeV data, we obtain the essential results shown in Table IV, resulting in values of Λ that can explain the 750 GeV diphoton excesses observed by both ATLAS [1] and CMS [2]. As we mentioned earlier, the extraction of Λ depends on what selection category is used. For the category of $2\gamma + 0j$ (C1) selection for ATLAS analysis, we get $\Lambda \approx 2.9$ TeV which can explain the excess. On the other hand we get slightly bigger $\Lambda \approx 4.2$ TeV for the selection category $\geq 2\gamma+ \geq 0j$ (C2). The corresponding CMS values on Λ are 3.2 TeV and 4.3 TeV for C1 and C2 respectively.

V.   CONCLUSIONS

In this paper we have proposed that the diphoton excess is due to a 750 GeV scalar associated with variations of the fine-structure constant. Our proposal predicts that the scalar dominantly decays to a photon pair, but has an appreciable branching ratio into a pair of fermions plus a photon, with BR($\phi \to \gamma q\bar{q}$) $\sim 13\%$ for quarks and BR($\phi \to \gamma \ell^+\ell^-$) $\sim 10\%$ for leptons. This gives the main additional prediction of our model: events with a lepton-lepton-photon resonance at 750 GeV.

The scalar resonance is dominantly produced together with an additional real or virtual photon, which, if virtual, gives rise to a pair of jets or leptons. This gives another prediction: the existence of an additional photon and/or jets in the events, which are not part of the resonance. These predictions should be looked for in future LHC analyses.

Our model has only two new parameters, the mass of the scalar m and the energy

13

scale Λ. Both are fixed by the LHC excess, with $m \sim 750$ GeV and $\Lambda \sim 3 - 4$ TeV.

It is interesting to note that the interaction terms for the new scalar are non-renormalizable. This means that the theory needs to be UV-completed, and as a consequence new physics is expected at the energy scale Λ. With our interpretation of the scalar as due to a moduli field parametrizing a varying electromagnetic coupling, natural candidates for this new physics are extra dimensions and possibly string theory. All of this would be within reach of the LHC.

Acknowledgments

[1] ATLAS Collaboration, *Search for resonances decaying to photon pairs in 3.2 fb^{-1} of pp collisions at $\sqrt{s} = 13$ TeV with the ATLAS detector*, Tech. Rep. ATLAS-CONF-2015-081 (2015).

[2] CMS Collaboration, *Search for new physics in high mass diphoton events in proton-proton collisions at 13TeV*, Tech. Rep. CMS-PAS-EXO-15-004 (2015).

[3] J. D. Bekenstein, Phys. Rev. **D25**, 1527 (1982).

[4] J. D. Bekenstein, Phys. Rev. **D66**, 123514 (2002), arXiv:gr-qc/0208081 [gr-qc] .

[5] J.-P. Uzan, Living Rev. Rel. **14**, 2 (2011), arXiv:1009.5514 [astro-ph.CO] .

[6] M. Zagermann, *Proc. Symposium From Varying Couplings to Fundamental Physics, JE-NAM 2010*, Astrophys. Space Sci. Proc. , 17 (2011).

[7] S. Knapen, T. Melia, M. Papucci, and K. Zurek, (2015), arXiv:1512.04928 [hep-ph] .

[8] D. Buttazzo, A. Greljo, and D. Marzocca, (2015), arXiv:1512.04929 [hep-ph] .

[9] R. Franceschini, G. F. Giudice, J. F. Kamenik, M. McCullough, A. Pomarol, R. Rattazzi, M. Redi, F. Riva, A. Strumia, and R. Torre, (2015), arXiv:1512.04933 [hep-ph] .

[10] S. Di Chiara, L. Marzola, and M. Raidal, (2015), arXiv:1512.04939 [hep-ph] .

[11] R. S. Gupta, S. Jäger, Y. Kats, G. Perez, and E. Stamou, (2015), arXiv:1512.05332 [hep-ph] .

[12] A. Falkowski, O. Slone, and T. Volansky, (2015), arXiv:1512.05777 [hep-ph] .

[13] L. Berthier, J. M. Cline, W. Shepherd, and M. Trott, (2015), arXiv:1512.06799 [hep-ph] .

[14] M. Chala, M. Duerr, F. Kahlhoefer, and K. Schmidt-Hoberg, (2015), arXiv:1512.06833 [hep-ph] .

[15] J. Bernon and C. Smith, (2015), arXiv:1512.06113 [hep-ph] .

[16] J. S. Kim, J. Reuter, K. Rolbiecki, and R. R. de Austri, (2015), arXiv:1512.06083 [hep-ph] .

[17] U. Danielsson, R. Enberg, G. Ingelman, and T. Mandal, work in progress (2016).

[18] D. Kimberly and J. Magueijo, Phys. Lett. **B584**, 8 (2004), arXiv:hep-ph/0310030 [hep-ph] .

[19] A. Alloul, N. D. Christensen, C. Degrande, C. Duhr, and B. Fuks, Comput. Phys. Commun. **185**, 2250 (2014), arXiv:1310.1921 [hep-ph] .

[20] J. Alwall, R. Frederix, S. Frixione, V. Hirschi, F. Maltoni, O. Mattelaer, H. S. Shao, T. Stelzer, P. Torrielli, and M. Zaro, JHEP **07**, 079 (2014), arXiv:1405.0301 [hep-ph] .

[21] J. Pumplin, D. R. Stump, J. Huston, H. L. Lai, P. M. Nadolsky, and W. K. Tung, JHEP **07**, 012 (2002), arXiv:hep-ph/0201195 [hep-ph] .

[22] J. de Favereau, C. Delaere, P. Demin, A. Giammanco, V. Lematre, A. Mertens, and M. Selvaggi (DELPHES 3), JHEP **02**, 057 (2014), arXiv:1307.6346 [hep-ex] .

[23] M. Cacciari, G. P. Salam, and G. Soyez, Eur. Phys. J. **C72**, 1896 (2012), arXiv:1111.6097 [hep-ph] .

[24] M. Cacciari, G. P. Salam, and G. Soyez, JHEP **04**, 063 (2008), arXiv:0802.1189 [hep-ph] .

[25] S. Fichet, G. von Gersdorff, and C. Royon, (2015), arXiv:1512.05751 [hep-ph] .

[26] C. Csaki, J. Hubisz, and J. Terning, (2015), arXiv:1512.05776 [hep-ph] .

[27] L. A. Anchordoqui, I. Antoniadis, H. Goldberg, X. Huang, D. Lust, and T. R. Taylor, (2015), arXiv:1512.08502 [hep-ph] .

[28] V. Khachatryan *et al.* (CMS Collaboration), Phys. Lett. **B750**, 494 (2015), arXiv:1506.02301 [hep-ex] .

[29] CMS Collaboration, *Search for High-Mass Diphoton Resonances in pp Collisions at*

sqrt(s)=8 TeV with the CMS Detector, Tech. Rep. CMS-PAS-EXO-12-045 (2015).

[30] G. Aad *et al.* (ATLAS Collaboration), Phys. Rev. **D92**, 032004 (2015), arXiv:1504.05511 [hep-ex] .

[31] G. Aad *et al.* (ATLAS Collaboration), Phys. Rev. Lett. **113**, 171801 (2014), arXiv:1407.6583 [hep-ex] .

[32] G. Aad *et al.* (ATLAS Collaboration), (2015), arXiv:1509.05051 [hep-ex] .